

A foveated passive UHF RFID system for mobile manipulation

Travis Deyle, Cressel Anderson, Charles C. Kemp, and Matthew S. Reynolds

Abstract— We present a novel antenna and system architecture for mobile manipulation based on passive RFID technology operating in the 850MHz-950MHz ultra-high-frequency (UHF) spectrum. This system exploits the electromagnetic properties of UHF radio signals to present a mobile robot with both wide-angle ‘peripheral vision’, sensing multiple tagged objects in the area in front of the robot, and focused, high-acuity ‘central vision’, sensing only tagged objects close to the end effector of the manipulator. These disparate tasks are performed using the *same* UHF RFID tag, coupled in two different electromagnetic modes. Wide-angle sensing is performed with an antenna designed for far-field electromagnetic wave propagation, while focused sensing is performed with a specially designed antenna mounted on the end effector that optimizes near-field magnetic coupling. We refer to this RFID system as ‘foveated’, by analogy with the anatomy of the human eye.

We report a series of experiments on an untethered autonomous mobile manipulator in a 2.5D environment that demonstrate the features of this architecture using two novel behaviors, one in which data from the far-field antenna is used to determine if a specific tagged object is present in the robot’s working area and to navigate to that object, and a second using data from the near-field antenna to grasp a specified object from a collection of visually identical objects. The *same* UHF RFID tag is used to facilitate both the navigation and grasping tasks.

I. INTRODUCTION

In simulation and in carefully controlled environments, robots can perform impressive feats of dexterous manipulation. Outside of these settings, robots have great difficulty performing basic tasks, such as picking and placing. A key reason for this discrepancy is the lack of reliable information about the state of the world in which the robot is operating [1]. Robotic sensory systems, such as cameras and microphones, produce signals that are difficult to interpret reliably and only indirectly provide information about critical aspects of the world, such as the identity, geometry, and pose of objects. Laser range finders have helped drive significant advances in mobility due to their effectiveness at perceiving the geometry of environments [2], but the inference of semantic information and object level information suitable for manipulation is an active area of research with significant challenges [3].

In this paper, we show that properly interpreted signals from UHF RFID tags on objects can serve as a powerful new sensory modality to enable mobile manipulation of tagged

T. Deyle and C. Anderson are with the Department of Electrical and Computer Engineering, Georgia Tech, Atlanta GA 30332

C. Kemp is with the Department of Biomedical Engineering, Georgia Tech, Atlanta GA 30332

M. Reynolds is with the Department of Electrical and Computer Engineering, Duke University, Durham NC 27708. e-mail: matt.reynolds@duke.edu

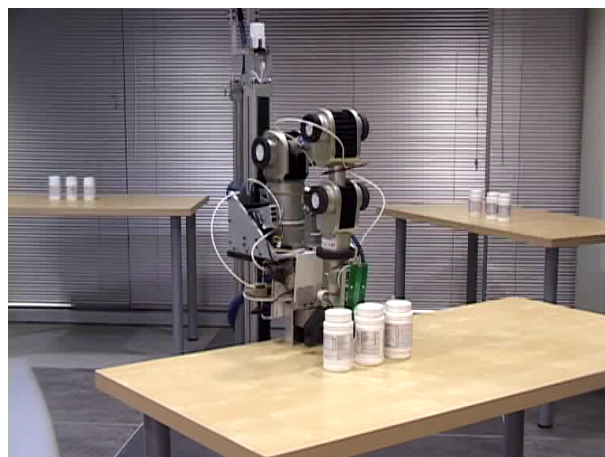


Fig. 1: Top: Robot using far-field mobility behavior
Bottom: Robot using near-field scan/grasp behavior

objects in otherwise uncontrolled environments. **We describe and evaluate a novel sensor architecture that uses the same UHF RFID tag attached to an object (in this case a pharmaceutical bottle) in two distinct modes of RF propagation to provide information critical to mobility and manipulation, respectively.** These two modes are the *near-field*, where the reader to tag distance d is small when compared to the $\approx 30\text{cm}$ UHF wavelength λ , and the *far-field*, where $d \gg \lambda$.

A far-field, wide-angle UHF antenna mounted to the mobile base provides long-range information about the identity, range, and heading of one specific tagged object among many, at read ranges of up to 5m. Our experiments show that signals received from a tagged object using this antenna are sufficient to enable navigation to the tagged object in an open area without the use of additional sensors.

We also show that a near-field UHF antenna mounted on the end effector has complementary capabilities. It provides short-range (cm to mm scale) information about the identity and range of the tagged object, which when coupled with a scanning behavior is sufficient to select and pick up a desired object surrounded by undesired tagged objects with identical external appearance. *The same passive UHF RFID tag is employed both in the near field and far field, so only a single object tag is required.*

The inspiration and name for this sensory configuration comes from the human eye, which has distinct sensing capabilities in the narrow-angle, high-resolution central part of the retina (the fovea) and the wide-angle, low spatial resolution periphery. In this paper, we characterize the foveated RFID sensors, present algorithms for their use, and validate their efficacy on an untethered, fully autonomous mobile manipulator.

II. RELATED WORK

There has been much recent interest in the application of passive RFID technology to robotics, in particular as a component of a robot's localization and mapping system. Several recent works employ long-range passive UHF (902-928MHz) RFID, in addition to a laser rangefinder and an odometry system, as sensor inputs to a probabilistic SLAM algorithm [7], [8], while others rely on short-range magnetostatically coupled passive RFID operating in the HF (13.56MHz) spectrum [6], [9]. Some automated parts-bin systems in the automotive industry use HF or LF (125KHz) RFID tags to identify specific parts bins [11]. Recent work in *active tagging* [10] demonstrates guidance to a battery powered target tag in a cluttered environment. In this work we demonstrate a UHF hybrid system in which long range tag communication is performed using far-field electromagnetic wave communication, while short range tag communication is performed using near-field, magnetic coupling. This is accomplished in both modes of operation *with the same low-cost passive tag*. The use of the same UHF RFID tag in both near-field and far-field modes is a unique capability of UHF tags that is previously unexploited in robotics applications. Because of the much lower operating frequency of LF and HF passive tags, they exhibit only near-field magnetic coupling and they cannot be used for long range operation as we demonstrate in this work. On the other hand, prior work with UHF tags has not leveraged their operation at very short ranges in the near-field regime. In this paper we present the first work combining the near-field and far-field information to facilitate mobile manipulation.

In the prior art in general, the passive RFID system has been used to provide identity information only; that is, the tag's stored data is either read or not read, and the resultant binary indication of presence is often used in a probabilistic formulation. In contrast, this work presents a methodology for using carefully chosen antenna radiation patterns in the far-field and near-field, in combination with minimum tag excitation power, to yield a continuous-valued statistic that is

an indicator of tagged object pose with respect to the reader antenna.

III. FOVEATED RFID SYSTEM ARCHITECTURE

The architecture of the foveated UHF RFID system for a mobile robot with manipulator is shown diagrammatically in Figure 2. A standard mobile robot base, the Erratic platform from Videre Design, Inc., is modified to include a 0.9m Z-axis translation stage carrying a Katana 6M 5DOF robotic arm with 0.55m horizontal reach and 0.75m vertical reach. The resulting mobile manipulator has a Z-axis stretch of up to 1.9m and can manipulate objects weighing up to 500g, sufficient for the type of small objects we wish to manipulate, such as medicine bottles, remote controls, and other small objects.

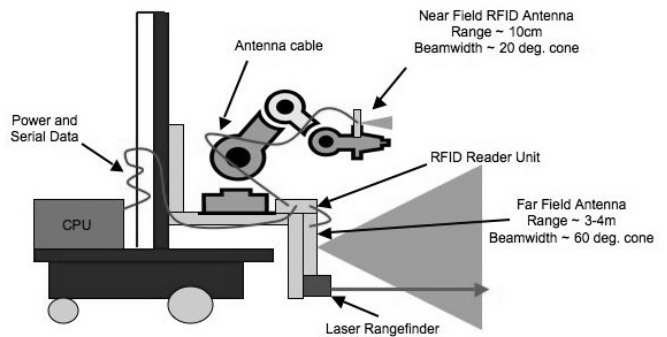


Fig. 2: The foveated RFID system mounted on the mobile manipulator

A. Passive RFID Tag Selection

The Alien Technology ALN-9540 UHF RFID tag, based on the ISO18000-6C communication protocol standard [4], is chosen for tagging the bottles used in our tests. The ISO18000-6C communication protocol (also called EPC Generation 2) is a widely adopted protocol supported by low cost tags (sub- $\$0.10$ USD) available from many manufacturers. These tags measure 95mm x 8.15mm x 0.5mm, and are fully passive, meaning they do not contain a battery because they derive their operating power from the RFID reader signal. The ALN-9540 contains 96 bits of read/write data storage, and a tag can be read in 1-3ms including communication protocol overheads. Because of the ISO18000-6C tag protocol's multi-tag arbitration algorithm, there is no limit to the number of tags that can be simultaneously present in the reader's interrogation zone. In our initial application, the 96 bit tag data storage contains a unique identifier, but with a larger tag IC memory space a full complement of pharmaceutical data could be stored as an XML record, for example.

The ALN-9540 passive tag exhibits a far-field antenna gain of approximately 0-1dBi, so its radiation pattern is roughly isotropic. To power up and operate properly, the tag requires an incident power across its terminals of approximately $50\mu\text{W}$, or -13dBm. This power requirement is the limiting

factor in the achievable read range for the tag, as will be shown later.

B. RFID reader selection and configuration

For this application, the ThingMagic Mercury4e RFID reader was selected because of its small size and low power consumption, requiring 9-12VDC at 1.5A maximum when reading tags, as compared to fully encased readers which typically require 24VDC at 2.5A or more. The Mercury4e module supports two antenna ports which are configured as shown in Figure 3.

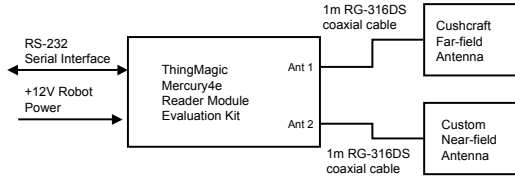


Fig. 3: RFID reader hardware configuration

The reader firmware is specified to read ISO18000-6C tags such as the ALN-9540 tags that were selected for this application, although the reader requires some configuration to select the protocol and RF power level. A driver implementing the power ramping algorithm shown in Figure 4 was written in Python to communicate with the reader module via RS-232 serial commands per the ThingMagic serial interface protocol, which is designed for polled mode interaction with the reader. This algorithm is used to find the minimum power at which the tag responds to the reader, a statistic that is valuable both in the near-field and far-field interactions.

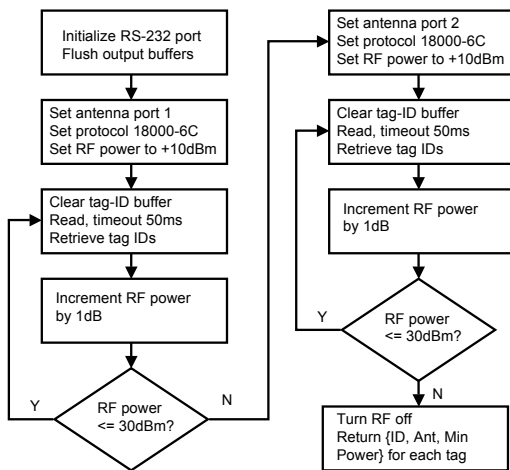


Fig. 4: RFID reader power ramping algorithm

IV. FAR-FIELD, WIDE ANGLE ANTENNA CHARACTERIZATION

In order to fully model the RFID system, it is necessary to characterize antenna performance as a function of tag pose relative to the antenna. In our system, the wide-angle antenna is designed to exhibit far-field electromagnetic coupling to

the tagged objects over a wide beamwidth. A flat panel antenna, model S9028PC12NF manufactured by Cushcraft Inc, is selected for this purpose. It is based on a half-wavelength air dielectric patch design [13]. This antenna is specified to provide 65° beamwidth in both the horizontal and vertical planes, with a peak gain of 7.5dBi, and has dimensions of approximately 25cm x 25cm x 4cm. The measured radiation pattern of this antenna is shown in Figure 5. The wide-angle antenna’s gain is specified in terms of its 3dB beamwidth, so the antenna gain is 7.5dBi on boresight and only 4.5dBi at the extremes of the 65° beamwidth. Because of this variation in antenna gain with offpointing angle, reading a tag requires a varying amount of reader power depending on tag pose with respect to the reader antenna. The next section explains how this effect can be modeled.

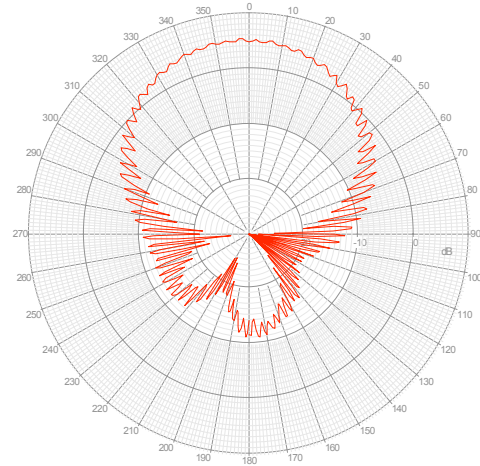


Fig. 5: Radiation pattern for wide-angle antenna, from [12]

A. Predicting far-field read range

To model far-field read range for the wide-angle antenna, we employ the ‘forward link limited’ assumption, meaning the tag will be readable at a given distance if it receives sufficient operating power from the RFID reader’s transmitted signal. This assumption is valid as long as the RFID reader’s receiver exhibits sufficient sensitivity to receive the tag’s backscattered reply signal at the tag’s incident power threshold.

To calculate the power incident on the tag, we start with the reader’s transmitted power P_{rdr} of 1.0W (+30dBm) and include the gain of reader and tag antennas G_{rdr} and G_{tag} , as well as free space path loss PL and cable loss $CL \approx 0.8dB$. If all these quantities are expressed in logarithmic units (dB) we can sum them as follows:

$$P_{tag} = P_{rdr} + G_{rdr} + G_{tag} - PL - CL \quad (1)$$

We then solve for PL_{max} , the path loss at the tag’s powerup threshold $P_{th} = -13dBm$:

$$PL_{max} = P_{rdr} + G_{rdr} + G_{tag} - P_{th} - CL \quad (2)$$

On boresight, where $G_{rdr} = 7.5\text{dBi}$, $PL_{max} = 50.7\text{dB}$. At the extreme of the antenna's beamwidth (32.5° off boresight), where $G_{rdr} = 4.5\text{dBi}$, $PL_{max} = 47.7\text{dB}$. To estimate maximum read distance given a path loss PL , we apply the Friis model [15], whose constants are derived from the spherical geometry of wave propagation. In this formulation of the Friis model, d is in meters and f is in MHz.

$$d = 10^{PL/20 - \log f + 1.378} \quad (3)$$

By setting the path loss PL in Equation 3 equal to the maximum tolerable path loss PL_{max} from Equation 2, we can estimate d_{max} , the reader to tag distance at the tag's powerup threshold. On boresight, $d_{max} = 8.9\text{m}$, while at 32.5° off boresight, $d_{max} = 6.3\text{m}$. In practice, measured indoor path loss is generally higher than that predicted by the Friis model due to the presence of absorptive materials and multipath induced fading [14], so the free space read range predictions should be taken as an upper bound.

1) *Measured far-field power versus distance*: A series of measurements of incident power at the tag were taken in an ordinary office environment, with reinforced concrete floors. Figure 6 clearly shows the effects of multipath propagation on the power received by the tag. At distances where incident power at the tag drops below the tag's powerup threshold, the tag cannot be read. In the particular environment where these measurements were performed, the tag may be read with 100% reliability at distances of up to 4m and is often, but not always, read at distances up to 6m. This is in good agreement with the predictions of the Friis model.

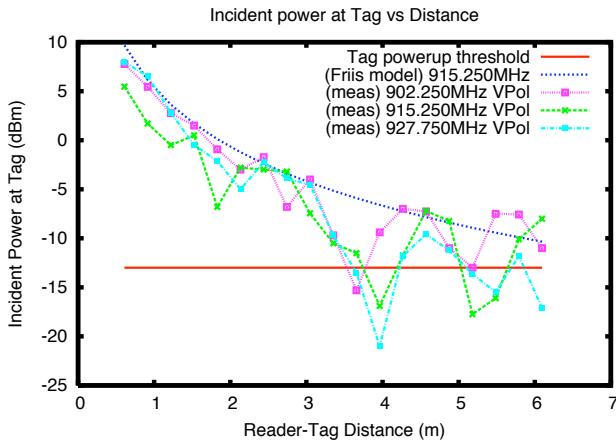


Fig. 6: Far-field measured incident power at the tag versus distance from wide-angle antenna, on boresight

2) *Measurement of far-field read power versus bearing to tag*: Figure 7 shows minimum read power versus bearing to a specific tag being read, at a distance of 2.13m. Because of the far-field radiation pattern shown in Figure 5, the bearing from the robot to the tag can be found by rotating the far-field antenna to achieve the minimum required read power. We have developed a mobility behavior to exploit this effect, presented in Figure 9, that can be used in an unobstructed environment to guide the robot from a starting point to a tag's location by means of successive update of robot heading.

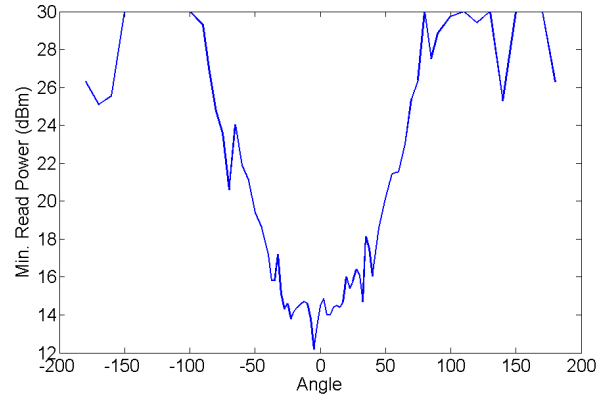


Fig. 7: Far-field measured minimum power to read tag 2.13m away, versus bearing to tag

V. NEAR-FIELD, MAGNETICALLY COUPLED ANTENNA CHARACTERIZATION

The near-field, magnetostatically coupled antenna, called a 'near-field coupler', is based on a printed circuit microstrip structure designed to emphasize the production of RF magnetic fields in close proximity to the coupler. By means of a flexible coaxial cable running along the robot's arm, the RFID reader unit is connected to the near-field coupler located at the manipulator's wrist joint. The near-field coupler is comprised of specially designed printed circuit board containing a terminated microstrip section of $1/4$ guided wavelength. When the passive tag is in proximity to the microstrip section, the fringing magnetic fields from the microstrip section couple to the small loop section of the ALN-9540 tag. The resulting near-field coupling exhibits a far-field gain of less than -13dBi , so it radiates approximately 20dB less (1%) of the energy radiated by the far-field antenna. This results in a correspondingly shorter read range for the near-field coupler. A far-field radiation pattern measurement is not useful for characterizing the near-field performance of the microstrip coupler, so we perform a near-field measurement by systematically moving the tag across the microstrip coupler and recording the minimum power required to read the tag.

Figure 8 shows measured near-field coupling, as determined by the minimum power required to read the tag, at each 10mm increment of translation from left to right across the near-field coupler, at varying tag to coupler separations. The near-field coupler exhibits a spatially selective coupling that results in the minimum read power occurring when the tag is aligned with the center of the coupler. The slope of minimum read power curve can be used to estimate tag to coupler distance. By moving the manipulator left-to-right across the sample region, the position of maximal coupling between the tag and the near-field coupler may be ascertained. As seen in Figure 8, this position of alignment corresponds to a spatial error of $\pm 1.0\text{cm}$ at a tag to coupler separation of 2cm. We expect that improved positioning accuracy can be achieved by further optimizing the near-field

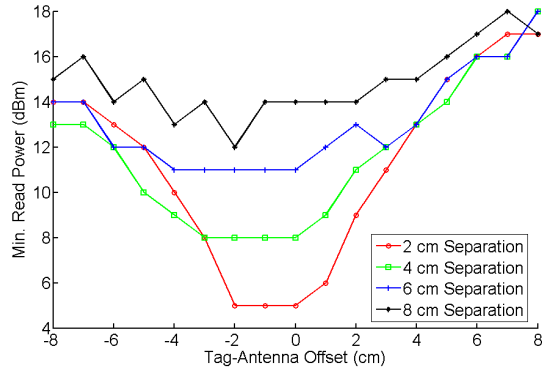


Fig. 8: Near-field minimum required power to read tag at different displacements and separation distances

coupler geometry.

VI. CONTROL SYSTEM AND BEHAVIORAL DESIGN

To demonstrate foveated sensing, both the near-field and the far-field UHF RFID sensing modalities were utilized in independent robot behaviors. The mobility behavior shown in Figure 9 is intended to navigate the robot from its starting location to a specified tag in an unobstructed environment. It takes advantage of the angular dependence of minimum read power as an indicator of robot to tag bearing as shown in Figure 7. This simplified behavior does not take into account the possible presence of obstacles along the shortest path between the robot and the tag. The results of a series of trials of the Figure 9 behavior in an unobstructed environment are presented in Section VII.

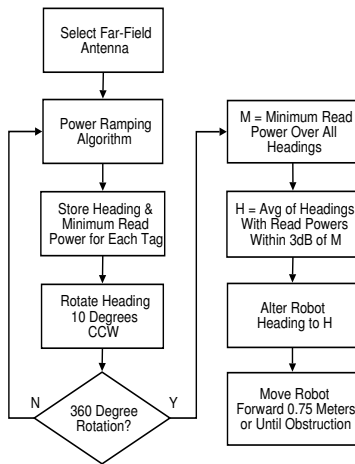


Fig. 9: Far-field behavior for mobility

Figure 10 presents a simplified behavior for grasping a specified, tagged object from a group of previously unknown objects in front of the robot. The robot's laser rangefinder gathers centroid data for each object within the workspace of the grasp controller. Then the near-field antenna, mounted on the end effector of the manipulator, is scanned from right to

left across the group of objects, maintaining a constant 2cm distance between the end effector and the laser-determined object centroid. The minimum read power is used to estimate object displacement in the plane of motion as shown in Figure 8. Once the specified object has been selected from the set of laser identified object centroids, the manipulator performs an overhead grasp on that object, using a grasp designed to match the object type based on the data read from the RFID tag. The results of a series of trials of this behavior in an unobstructed environment are presented in Section VII.

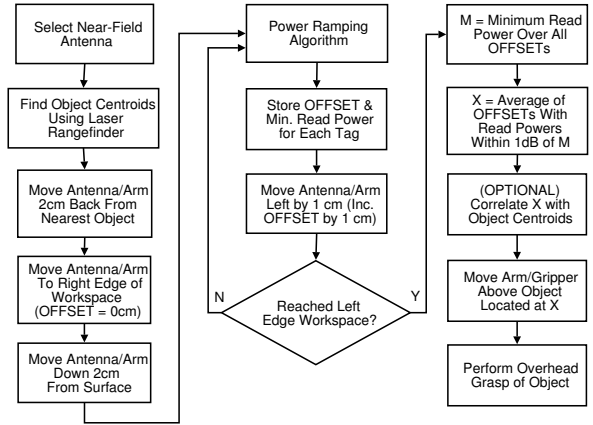


Fig. 10: Near-field behavior for grasping

VII. ON-ROBOT EVALUATION

Our evaluation scenario is motivated by the assistive robotics problem of locating and grasping selected objects in a home environment, and bringing them back to a disabled person. In this scenario we have tasked the mobile manipulator with locating and grasping a specified tagged plastic medication bottle from among nine visually identical, tagged plastic medication bottles placed on three different tables in an unobstructed environment (see Figure 1). The three bottles on each table are closely spaced ($\approx 2\text{cm}$) in groups, and the three tables are evenly spaced on a circle of $\approx 3\text{m}$ diameter. One of the tagged bottles is designated as the target for mobility and for grasping. The US Food and Drug Administration (FDA) has recently introduced an electronic drug pedigree initiative [5] through which RFID tags will be phased in on prescription labels, so this application may soon become particularly relevant. We tested each behavior five times from random starting locations.

A. Mobility Behavior Results

For each trial the robot executed the mobility behavior of Figure 9 starting from a random initial location and heading within the circle. The robot successfully maneuvered within a few centimeters of the correct table in four of five tests (80% success), with the only failure occurring when the initial starting location was beyond the tag's nominal read range (approximately 3.5 meters as shown in Figure 6).

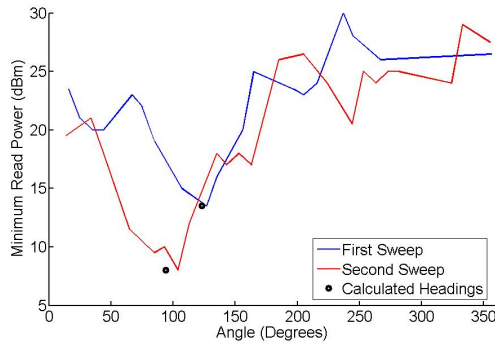


Fig. 11: Results of two 360 degree scans to find heading to target tag

The results of two 360-degree tag bearing scans taken with 1m robot motion during a single trial are presented in Figure 11, which also shows calculated target heading from each of the two scans.

B. Grasping Behavior Results

The robot was located in front of three visually identical bottles, lined up ≈ 2 cm apart within the manipulation workspace. One of the tagged bottles was randomly chosen for grasping. In all five trials (100% success), the robot identified and grasped the correct bottle. Figure 12 shows correlation data for two different bottles between object centroid found by the laser rangefinder, with the tag location determined by the near-field RFID system. Agreement to within 1cm is observed in these cases.

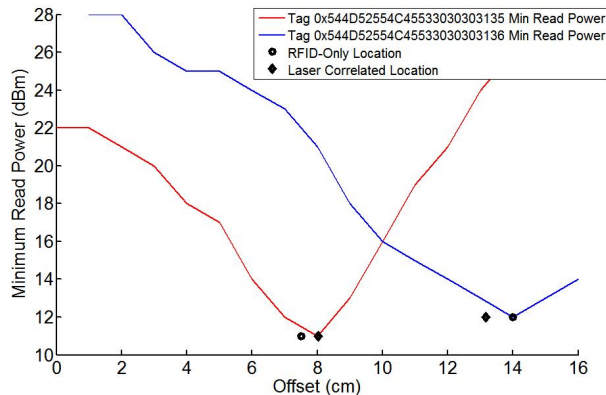


Fig. 12: Laser and near-field RFID object centroids

VIII. CONCLUSION

In this work we have demonstrated the first *foveated passive UHF RFID system* for mobile manipulation, in which a *single* passive UHF RFID tag on an object is sufficient for navigation toward a specified object over distances of over 3m, as well as near-field identification and grasping of an object within a distance of a few centimeters from an end effector. A specified tagged object can be uniquely addressed and identified even among hundreds of others,

limited only by the 96 bit ID space. Identification of tagged objects typically requires 1-3 ms, comparable to a typical laser scan. We have shown that properly interpreted signals from RFID tags on objects in both the near-field and far-field propagation modes can serve as a powerful new sensory modality to enable mobile manipulation of tagged objects. Our tests were autonomous and fully untethered, with all sensing and computation performed on-board.

We expect that the use of passive UHF RFID will become increasingly prevalent in robotics applications, especially those in the healthcare domain where medication is tagged by FDA mandate. The increasing capabilities and decreasing cost of UHF RFID tags will lead to their application in many other domains. We have shown that in addition to the detection of tag ID, passive RFID signals can be interpreted to provide valuable range and bearing information as well. This work presents the first on-robot exploitation of simultaneous interpretation of near-field and far-field signals from a single UHF RFID tag attached to an object, and the first use of those signals in mobile manipulation.

REFERENCES

- [1] C. C. Kemp, A. Edsinger, and Eduardo Torres-Jara, "Challenges for Robot Manipulation in Human Environments". *IEEE Robotics & Automation Magazine*, vol. 14 no. 1, pp. 20-29, March 2007.
- [2] S. Thrun, W. Burgard, and D. Fox, "Probabilistic Robotics". MIT Press, 2005.
- [3] A. Ranganathan and F. Dellaert, "Semantic Modeling of Places using Objects". *Robotics: Science and Systems (RSS)*, 2007.
- [4] EPC Global US, Class 1 Generation 2 UHF RFID Protocol for operation at 860MHz-960MHz, version 1.0.9, available online. <http://www.epcglobalus.org/>
- [5] United States Food and Drug Administration, Report on Combating Counterfeit Drugs, available online http://www.fda.gov/oc/initiatives/counterfeit/report02_04.html
- [6] O. Kubitz, M. O. Berger, M. Perlick, and R. Dumoulin, "Application of radio frequency identification devices to support navigation of autonomous mobile robots", in *Proceedings of IEEE 47th Vehicular Technology Conference*, pp.126-130, 4-7 May 1997
- [7] D. Hahnel, W. Burgard, D. Fox, K. Fishkin, M. Philipose, "Mapping and localization with RFID technology", in *Proceedings of 2004 IEEE International Conference on Robotics and Automation*, pp. 1015-1020, 26 April-1 May 2004
- [8] S. Roh, Y.H. Lee, H.R. Choi, "Object Recognition Using 3D tag-based RFID System", in *Proceedings of 2006 IEEE/RSJ International Conference on Intelligent Robots and Systems*, pp. 5725- 5730, Oct. 2006
- [9] V.A. Ziparo, A. Kleiner, B. Nebel, D. Nardi, "RFID-Based Exploration for Large Robot Teams" in *Proceedings of 2007 IEEE International Conference on Robotics and Automation* pp.4606-4613, 10-14 April 2007
- [10] M. Kim; H. Kim; N. Chong, "Automated Robot Docking Using Direction Sensing RFID" in *Proceedings of 2007 IEEE International Conference on Robotics and Automation*, pp.4588-4593, 10-14 April 2007
- [11] Escort Memory Systems, Inc. Automotive Applications, available online <http://info.ems-rfid.com/mainmenu1/applications/automotive/index.html>
- [12] Cushcraft Inc. S9028PC12NF antenna datasheet, available online. <http://www.cushcraft.com/support/pdf/S9028PC12NF.pdf>
- [13] C. A. Balanis, *Antenna Theory: Analysis and Design*, 3rd Ed., New Jersey: John Wiley and Sons, 2005. pp. 816-843.
- [14] S.Y. Seidel and T.S. Rappaport, "914MHz path loss prediction models for indoor wireless communications in multifloored buildings". *IEEE Transactions on Antennas and Propagation*, vol. 40 no. 2, February 1992, pp. 207-217.
- [15] D. M. Pozar, *Microwave Engineering*, 4th Ed., New Jersey: John Wiley and Sons, 2004, p. 648.